Source-Free Domain Adapation for Image Segmentation

Mathilde Bateson[1] MATHILDE.BATESON.1@ENS.ETSMTL.CA
[1] *ETS Montreal*
Hoel Kervadec[1]
Jose Dolz[1]
Hervé Lombaert[1]
Ismail Ben Ayed[1,2]
[2] *CRCHUM, Montreal*

Editors: Under Review for MIDL 2022

Abstract

Domain adaptation (DA) tackles the performance drop observed when applying a model on target data from a different domain than the training one. However, most common DA techniques require concurrent access to the input images of both the source and target domains, which is often impossible for privacy concerns. We introduce a source-free domain adaptation for image segmentation, leveraging a prior-aware entropy minimization. We validate on spine, prostate and cardiac segmentation problems. Our method yields comparable results to several state-of-the-art adaptation techniques, despite having access to much less information. Our framework can be used in many segmentation problems, and our code is publicly available at https://github.com/mathilde-b/SFDA

Keywords: Segmentation, source-free domain adaptation

1. Introduction

A major impediment for the deployment of deep Convolutional Neural Networks (CNNs) in medical imaging is that they are seriously challenged by domain shifts between scans from different vendors, machines, modalities and acquisition protocols. To improve the performance of models across domains, recent works have focused on leveraging deep adversarial training to extract domain invariant features from input images. These methods either follow a generative approach, by transforming images from one domain to the other, or minimize the discrepancy in the feature and/or output spaces learnt by the model (Tsai et al., 2018). One major limitation of these approaches is that, by design, they require concurrent access to both the source and target data during the adaptation phase. Relieving from this constraint, and closest to our work, test-time domain adaptation (TTA) was introduced to improve generalization to new and different data, possibly a single data point, at test time (Karani et al., 2021; Wang et al., 2021).

We propose a *Source-Free Domain Adaptation* formulation (SFDA). A longer version of this teaser document is available at (Bateson et al., 2021b). Our formulation is based on a minimization of a label-free Shannon entropy loss ℓ_{ent} defined over the target-domain data, which we further guide with a domain-invariant prior on the segmentation regions sizes for each foreground class k, with $0 < k \leq K$. Given a set of images in the target domain, $I_t : \Omega_t \subset \mathbb{R}^2 \rightarrow \mathbb{R}$, $t = 1, \ldots, T$, our method minimizes the following loss during the adaptation phase: $\min_\theta \quad \sum_t \frac{1}{|\Omega_t|} \sum_{i \in \Omega_t} \ell_{ent}(\mathbf{p}_t(i, \theta)) + \mathrm{KL}(\widehat{\tau}(t, \theta, \cdot), \tau_e(t, \cdot))$, where

Table 1: Performance of the domain adaptation methods in terms of DSC(%) and ASD(vox)

Method	Source Free	Spine IVDs DSC	Spine IVDs ASD	Prostate DSC	Prostate ASD	Cardiac DSC	Cardiac ASD
NoAdap (lower bound)	✓	68.5	2.15	67.2	10.59	38.8	14.6
Oracle (upper bound)	✓	87.5	0.38	88.4	1.81	89.2	3.0
AdaptSegNet (Tsai et al., 2018)	×	**82.4**	**0.50**	**83.1**	**2.43**	**74.2**	**5.2**
AdaSource (Zhang et al., 2019)	×	75.9	0.99	76.3	3.93	70.7	7.6
CDA (Bateson et al., 2021a)	×	75.7	0.86	77.9	3.28	71.4	5.9
TTA (Karani et al., 2021)	✓	69.7	1.65	73.2	**3.80**	40.7	12.9
Tent (Wang et al., 2021)	✓	68.8	1.84	68.7	5.87	48.2	11.2
Prior AdaEnt (Bateson et al., 2020)	✓	72.9	1.54	77.8	4.10	65.6	8.2
AdaMI (Ours)	✓	**74.2**	**1.17**	**79.5**	3.92	**75.7**	**5.6**

$\mathbf{p}_t(i,\theta) = \left(p_t^1(i,\theta), \ldots, p_t^K(i,\theta)\right) \in [0,1]^K$ are softmax predictions of the target, $\tau_e(t,k)$ is a class-ratio estimate derived from anatomical prior knowledge (see Appendix of (Bateson et al., 2021b) for more details), and $\widehat{\tau}(t,k,\theta) = \frac{1}{|\Omega_t|}\sum_{i\in\Omega_t} p_t^k(i,\theta)$ is the class-ratio of the network output prediction.

2. Experiments and Results

Datasets – 3 datasets were used. **IVDM3Seg:** This spine dataset consists of 16 3D multi-modal MRIs. We set the water modality (Wat) as the source and the in-phase (IP) modality as the target domain. 12 scans are used for training, one for validation, and the 3 scans for testing. **NCI-ISBI13:** This prostate dataset consists of 30 volumes 3T MRI Siemens scanner (source) and 30 volumes generated with a 1.5T Philips Achieva (target). We use 19 scans for training, one for validation, and 10 scans for testing. **MMWHS:** This cardiac dataset consists of 20 MRI (source) and 20 CT (target). We used 14 subjects used for training, 2 for validation, and 4 for testing. For all datasets, images are normalized to zero mean and unit variance. We performed a data augmentation based on affine transformations.

Benchmark methods – We compare our proposed model *AdaMI* to the DA methods (Bateson et al., 2020, 2021a; Zhang et al., 2019; Tsai et al., 2018), and to two source-free domain adaptation methods: TTA (Karani et al., 2021), and Tent (Wang et al., 2021).

Training and evaluation details – The adaptation phase is initialized with the network parameters $\tilde{\theta}$ obtained from the fully supervised source training phase. We employed UNet, trained with the Adam optimizer, for 150 epochs, an initial learning rate of 1×10^{-6}, a weight decay of 10^{-3}, and a batch size of 24. We use the 3D Dice similarity coefficient (DSC) and the 3D average symmetric surface distance (ASD) as evaluation metrics.

Results – Table 1 presents our quantitative results. On spine (resp. prostate) images, our model *AdaMI* reaches a DSC score of 74.2% (resp. 79.5%), representing 90% (resp. 95%) of the best-performing adaptation method, *AdapSegNet*. Surprisingly, on cardiac images, where the domain shift is higher, *AdaMI* ranks best out of other DA adaptation techniques. On all three applications, *AdaMI* outperforms the two other source-free domain adaptation methods. The visual results in Fig 1 confirm the ability of *AdaMI* to produce

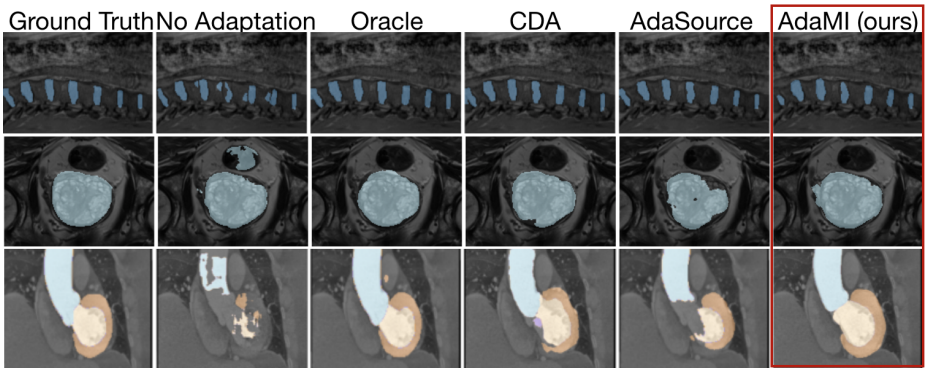

Figure 1: Visual results on spine (top) prostate (middle), and cardiac (bottom) images.

accurate predictions, with regular edges (see top row), and to recover foreground structures which had been missed without adaptation (see bottom row).

3. Conclusion

We tackle source-free domain adaptation (SFDA) for semantic segmentation. Our formulation achieves a better performance on cardiac, spine and prostate than SFDA methods, and comparable performance than state-of-the-art methods which need access to source data.

Acknowledgments – This work was supported by NSERC, FRQNT, the Canada Research Chair in Shape Analysis, and the ETS Chair on AI in Medical Imaging.

References

M Bateson, H Kervadec, J Dolz, H Lombaert, and I Ben Ayed. Source-relaxed domain adaptation for image segmentation. In *MICCAI*, 2020.

M. Bateson, J. Dolz, H. Kervadec, H. Lombaert, and I. Ben Ayed. Constrained domain adaptation for image segmentation. *IEEE TMI*, 2021a.

M Bateson, H Kervadec, J Dolz, H Lombaert, and I Ben Ayed. Source-free domain adaptation for image segmentation. 2021b. URL https://arxiv.org/abs/2108.03152.

N. Karani, E. Erdil, K. Chaitanya, and E. Konukoglu. Test-time adaptable neural networks for robust medical image segmentation. *Medical Image Analysis*, 2021.

Y. Tsai, W. Hung, S. Schulter, K. Sohn, M. Yang, and M. Chandraker. Learning to adapt structured output space for semantic segmentation. *CVPR*, 2018.

D Wang, E Shelhamer, S Liu, B Olshausen, and T Darrell. Tent: Fully test-time adaptation by entropy minimization. In *ICLR*, 2021.

Y Zhang, Philip D, Hassan F, and Boqing G. A curriculum domain adaptation approach to the semantic segmentation of urban scenes. *IEEE TPAMI Intelligence*, 2019.